Polymer 55 (2014) 1716–1723

Contents lists available at ScienceDirect

Polymer

journal homepage: www.elsevier.com/locate/polymer

Macromolecules of poly-(12-acryloylaminododecanoic acid) in organic solvent: Synthesis and molecular characteristics

N.V. Tsvetkov [a,*], E.V. Lebedeva [a], A.A. Lezov [a], A.N. Podseval'nikova [a], L.I. Akhmadeeva [a], I.M. Zorin [b], A. Yu Bilibin [b]

[a] Department of Physics, St. Petersburg State University, Ul`janovskaja Street 1, St. Petersburg, 198504 Russia
[b] Department of Chemistry, St. Petersburg State University, Universitetskij Prospect 26, St. Petersburg, 198504 Russia

ARTICLE INFO

Article history:
Received 22 January 2014
Accepted 5 February 2014
Available online 14 February 2014

Keywords:
Comb-like polymer
Macromolecule conformation
Optical anisotropy

ABSTRACT

The samples of poly(12-acryloylaminododecanoic acid) were synthesized in micellar solutions of the monomer. The possibility of obtaining polymeric ionogenic surfactants of different molecular masses by varying concentration of monomeric surfactant was demonstrated. Detailed studies of the obtained polymer were performed using macromolecular hydrodynamic methods, dynamic light scattering, scanning probe microscopy and flow birefringence. The parameter of equilibrium rigidity of macromolecules (the Kuhn segment length $A = 62 \times 10^{-8}$ cm) and their effective hydrodynamic diameter were determined in mixed solvent (dioxane-cyclohexanol). Contributions made by optical microform and macroform effects to the observed dynamic birefringence were analyzed in detail. The intrinsic optical anisotropy of the monomer unit was estimated; it correlates well with the corresponding values for comb-shaped polymers of similar structure.

1. Introduction

Monomers and polymers capable of self-organization in dilute solutions are very interesting objects for fundamental science; besides, they also have great practical value due to their possible applications as surface-active micelle-forming agents, stabilizers for disperse systems, flocculants and drug carriers. There are several architectures of self-organizing monomers; the most convenient one is a classical ionic surfactant having linear hydrophobic part with ionic group attached to one end and polymerizable fragment attached to another end. These monomers undergo free-radical polymerization in micellar solutions to give "polymerized micelles" or comb-shaped polyelectrolytes capable of intramolecular hydrophobic association in water. Polymerization of micelle-forming monomers is a promising way for the synthesis of well-organized macromolecules and nanoparticles. Polymerizable ionic surfactant molecules and "polymerized micelles" obtained from them can be considered as building blocks in design of complex macromolecular objects being at once molecules and nanoparticles. So far a large number of papers on synthesis and polymerization of anionic [1–7] and cationic [8–14] micelle-forming monomers, and studies of "polymerized micelles" in aqueous solutions [15–21] have been published. However, little attention is paid to the specific behavior of these polymers in the nonionized state in organic solvents.

Hydrodynamic characteristics of comb-shaped molecules can be used in determining equilibrium rigidity of their main chains. Flexibility of the main chain decreases a little with increasing length of side moiety; this effect may be explained by the interaction between side chains which becomes stronger with increasing side chain length [22]. The method of dynamic light scattering allows getting information about the of the particles under investigation in water [23–25], and in other environments [26]. Flow birefringence studies of solutions of comb-shaped polymers allow us to obtain additional important information about conformational characteristics of both main and side chains, since the value and sign of anisotropy of the whole macromolecule are largely determined by the structure and anisotropy of its side radicals [27,28].

Recently we have published a number of papers concerning synthesis and studies of poly(11-acryloylaminoundecanoic acid) (PAAUA) and its cross-linked analogue in organic media [29]. It was found that these polymer chains possess rather high equilibrium rigidity ($A \approx 10$ nm). We have supposed that this phenomenon is caused by the presence of amide groups in side moieties of PAAUA macromolecules which are directly linked to the main polymer chain.

* Corresponding author. Tel.: +7 812 428 46 66.
E-mail address: N.Tsvetkov@mail.ru (N.V. Tsvetkov).

http://dx.doi.org/10.1016/j.polymer.2014.02.019
0032-3861/

The present work is focused on the investigation of a novel polymer synthesized from a micelle-forming monomer sodium 12-acryloylaminododecanoate. Comprehensive studies of poly(12-acryloylaminododecanoic acid) (PAADA) with long aliphatic fragment attached to the main chain via amide group were performed using molecular hydrodynamic and optical methods. The purpose of the investigation was to reveal mechanism of influence of side chains on physical parameters of macromolecules.

2. Experimental section

2.1. Materials

12-aminododecanoic acid and acryloyl chloride were purchased from Sigma–Aldrich.

2.1.1. Monomer synthesis and polymerization

The solution of 0.028 mol of acryloyl chloride in 5 ml of carbon tetrachloride was added drop-wise to a solution containing 0.023 mol of 12-aminododecanoic acid, NaOH (0.05 mol) and 5 ml of *n*-butanol in 50 ml of water; the procedure was carried out for 20 min under vigorous stirring and cooling with cold water bath. After addition of all acryloyl chloride solution, stirring was continued for 30 min at pH not less than 8; then the mixture was acidified with 2.5 ml of concentrated HCl. 12-Acryloylaminododecanoic acid was collected by filtration, washed with water, dried and crystallized from ethyl acetate. The yield was 82% and the melting point of the product was 96–98 °C.

Sodium salt of 12-acryloylaminododecanoic acid was obtained by dissolving 1.51 g (0.0056 mol) of the above acid in 20 ml of methanol containing 0.225 g (0.0056 mol) of NaOH, filtered and precipitated by pouring in large excess of acetone. Precipitate was filtered, washed with acetone and pentane, dried in vacuum desiccator over $CaCl_2$ and stored in desiccator over sulfuric acid. The yield was 82% and melting point was 220–222 °C. The results of elemental analysis were the following: calculated C% 61.83; H% 8.99; N% 4.81; Found C% 61.83; H% 9.50; and N% 4.79.

Typical procedure of polymerization was performed as follows: AAD-Na (300 mg) was dissolved in an appropriate amount of water to obtain the desired monomer concentration (ranging from 0.005 to 0.2 mol/L). Potassium persulfate was added to reach its concentration 1 g/L, and argon was bubbled through the reaction mixture for 15 min. Polymerization proceeded for 1 h in a thermostated bath at 60 °C, and product was isolated by pouring the reaction mixture into 100 ml of 0.5 N HCl. To isolate polymer as a Na-salt, precipitation in acetone was used. Polymer was washed with water and dried in desiccator over sulfuric acid. Polymerization runs carried out at various monomer concentrations yielded polymers with different degrees of polymerization.

Sodium salt of 12-acryloylaminododecanoic acid is a micelle-forming monomer, the next higher homolog of well-described 11-acryloylaminoundecanoic acid (AAU-Na). We did not try to measure CMC of AAD-Na supposing it should be 2–3 times lower than that of AAU-Na (4×10^{-4} mol/L) [6]. For AAU-Na, the existence of bilayered structures in solution, such as vesicles and tubules, was shown [30]; it can be expected that AAD-Na will demonstrate similar behavior. Even at high concentrations, monomer solutions were clear (or slightly turbid if contained a fraction of monomer in acid form) and non-viscous. Polymerization is characterized by a long induction period (up to 30 min depending on monomer concentration); after that, nearly 100% conversion is reached in a few minutes. All polymer solutions were clear and viscous.

The structure of monomer unit is given in Fig. 1.

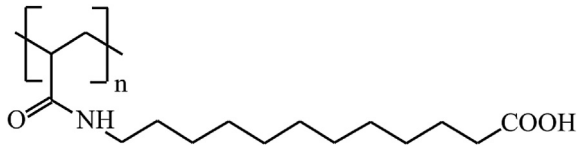

Fig. 1. Structural formula of PAADA monomer unit.

Fig. 2 presents conversion curves for processes carried out at various initial monomer concentrations (conversions were determined by spectrophotometry). The initial polymerization rates estimated using these curves were (567, 237, 113, 9) $\times 10^{-4}$ mol/(L $\times$ min) at monomer concentrations of 0.2, 0.1, 0.05 and 0.01 mol/L, respectively. These data were used to determine the reaction order with respect to monomer (1.4). This value of the reaction order can be explained by low initiator efficiency. The monomer is present in the reaction mixture in the micellized state, the micelles possessing negative surface charge. The concentration of free monomer does not exceed CMC, i.e. is about 10^{-4} mol/L. In these conditions, initiation by negatively charged primary SO_4^- radicals can be realized only during interaction of radicals with free monomer molecules; thus, it is indeed ineffective. Chain growth starts after transferring the formed monomeric or oligomeric radical into monomer micelle and proceeds very fast with the formation, first, of polymer–monomer particle and then of "polymerized micelle". Depending on molecular mass and concentration of the solution, PAAD-Na molecules can probably have various conformations (from micelle-like globules to loose coils); this process is controlled by competition between hydrophobic and charge interactions and requires special consideration.

Fig. 3(a–c) illustrates the data, observed by AFM for PAAD-Na molecules (analogues of PAADA-5 in Table 1) after rapid adsorption on mica surface from the solution at a concentration of 0.02 g/L. The AFM images show particles, similar to a hard sphere. Images allow us to determine the size of objects: the average height of $h = 1.8$ nm and a base diameter of $r = 80$ nm. This makes it possible to estimate the volume and molecular weight of the particles. Using the well-known equation for the volume segment of a sphere: $V = \pi \times h \times (3r^2 + h^2)/6$, where h is the height of the segment and r the diameter of its base, we can find the volume of the particle $V = 4530$ nm^3. Thus the molecular weight of the particles can be assessed as $M = \rho V N_A = 2.7 \times 10^6$, assuming the particle density ρ close to 1 g/cm^3. Taking into account the molecular weight of the macromolecule (see Table 1) we can assume that the observed particles at the AFM images are associates of approximately 4 macromolecules.

All studies of the polymer in the polyacid form were made in the mixed solvent (dioxane/cyclohexanol, volume ratio 1:1). Two

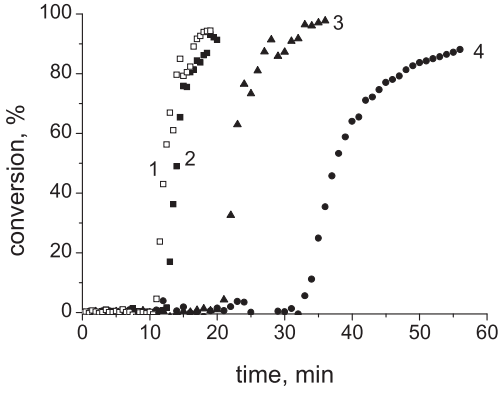

Fig. 2. Time-conversion curves for AAD-Na monomer at various concentrations: 1 – 0.2 mol/L; 2 – 0.1 mol/L; 3 – 0.05 mol/L; and 4 – 0.01 mol/L.

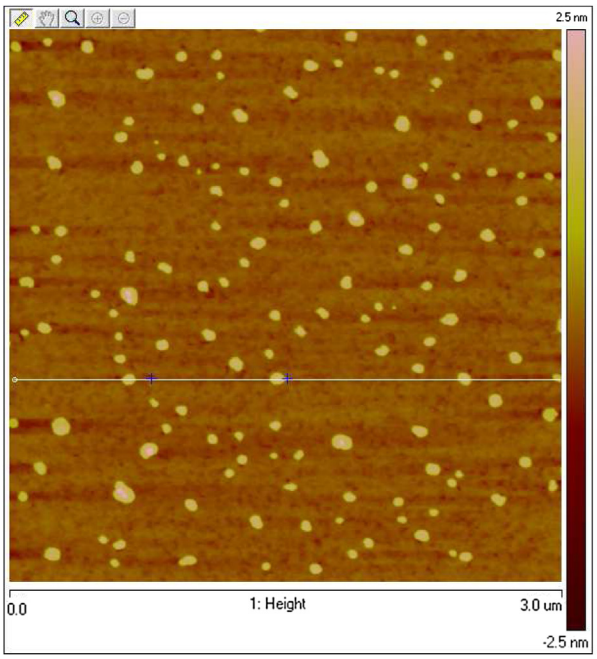

(a)

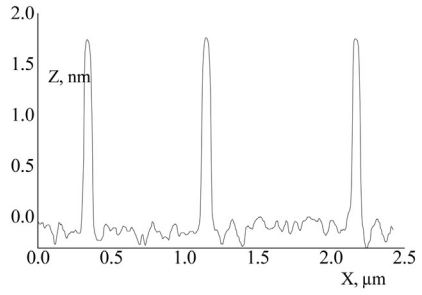

(b)

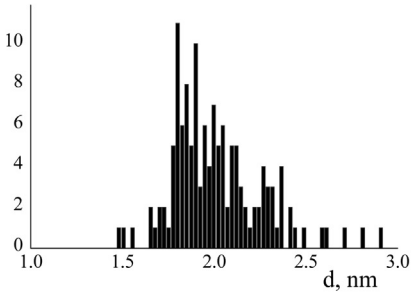

(c)

Fig. 3. (a) AFM image of PAAD-Na (image size 3 × 3 μm, *Z*-scale 5 nm) (deposited from aqueous solution ($c = 0.02$ g/L) onto mica plate, exposure for 1 min + spin-coating); (b) line profile; and (c) height distribution.

solvents with the following parameters were used: refractive index $n_s = 1.4385$, density $\rho = 0.9793$ g/cm^3, dynamic viscosity $\eta_0 = 2.69$ cP, and $n_s = 1.4375$, $\rho = 0.9795$ g/cm^3, $\eta_0 = 2.28$ cP. Cyclohexanol was chosen as a solvent due to high solubility of the studied samples in it; however, since this alcohol possesses rather high viscosity and high crystallization temperature ($T_c = 20$ °C), we decided to mix it with dioxane at a volume ratio of 1:1.

All studied polymer solutions were completely transparent and colorless within the used concentration ranges. Immediately before measurements, polymer solutions were filtered through Sigma–Aldrich filters (pore diameter 1 μm).

2.2. Methods

The intrinsic viscosities [η] were measured using the Ostwald capillary viscometer according to the standard technique [27]. In the capillary viscometers, outflow time for the pure solvent was from 90 to 115 s. The temperature during measurements was 24 °C. The error of the solution viscosity measurements did not exceed 5%.

Dynamic light scattering experiments were carried out using a "PhotoCor Complex" (Photocor Instruments, Inc., Moscow, Russia) apparatus. It comprised a digital correlator (288 channels, 10 ns), standard goniometer (10–150°), and a thermostat with temperature stabilization of 0.05 °C.

Two single-mode solid-state linear polarized lasers ($\lambda_0 = 405$ and 654 nm) served as an excitation source. The experiments were carried out at scattering angles ranging from 30° to 130°. The normalized intensity homodyne autocorrelation functions were fitted by the ILT regularization procedure incorporated in "DynaLS" software providing the relaxation time and hydrodynamic radius distributions. As all the observed modes displayed diffusion nature ($1/\tau = D \cdot q^2$), the values of the translation diffusion coefficients D were calculated from the slope of linear dependence of the relaxation rate $1/\tau$ versus the scattering vector squared, $q = 4\pi n_0/\lambda_0 \sin(\theta/2)$.

The hydrodynamic size distribution is an intensity-weighted one. For this kind of distribution, the area ω_i of peak i does not provide information about the concentration of each type of particles in the solution. Large particles scatter light more efficiently than small ones, which results in enhancement of the peak area for intensity-weighted distribution function. The mass distributions X_i for aggregates and single molecules were estimated using the following relationship [31]

$$X_i = \left(\omega_i / R_{h_i}^2\right) \Big/ \sum_i \omega_i / R_{h_i}^2. \quad (1)$$

Here, ω_i is the intensity-weighed peak area, $R_{h_i} = kT/6\pi\eta_0 D_i$ is the hydrodynamic radius of the corresponding particle, which calculated using Stokes–Einstein equation.

Weight-average molecular masses M_w of PAADA samples were found via static light scattering in D + C solutions using the following equation:

$$\left(\frac{H_c}{R_\theta}\right)_{\theta \to 0} = \frac{1}{M_w} + 2A_2 c, \quad (2)$$

where $H = 4\pi^2 n_0^2/(N_A \lambda^4)(\Delta n/\Delta c)^2$, R_θ is the Rayleigh ratio, A_2 is the second virial coefficient. The $(H_c/R_\theta)_{\theta \to 0}$ values were obtained through the linear extrapolation of the corresponding dependences to zero scattering angle θ at a finite value of solution concentration.

Table 1
Values of intrinsic viscosity [η], the Huggins constant K', translational diffusion coefficient D, hydrodynamic radius R_h, molecular mass M, refractive index increment dn/dc and optical shear coefficient $\Delta n/\Delta\tau$ for different PAADA samples in the mixed solvent (D + C).

Ser. No.	[η], cm^3/g	K'	$D \times 10^8$, cm^2/s	R_h, nm	$M \times 10^{-4}$	dn/dc	$\Delta n/\Delta\tau \times 10^{10}$, cm × s^2/g
1	20	0.62	17	5.6	8[a]	–	–
2	35	0.29	12	8.0	13[a]	0.10	−8.1
3	82	0.27	4.6	17.6	60	0.07	−4.4
4	86	0.52	4.4	18.4	61	0.07	−4.9
5	46	0.58	5.3	15.3	68	–	–
6	69	0.26	5.0	16.2	90[a]	0.10	−4.2
7	135	0.33	3.4	23.9	93	–	−4.4
8	49	0.64	4.6	17.6	97	0.07	–
9	97	0.17	3.4	23.9	126	0.06	–

[a] Calculated at $\eta_0 = 2.28$ cP.

The refractive indices of the solutions and solvents were determined using a METTLER TOLEDO refractometer (RM40 model, Switzerland) to an accuracy of $10^{-4} \pm 5 \times 10^{-5}$.

Density measurements were carried out using a METTLER TOLEDO density meter (DM40 model, Switzerland) to an accuracy of $10^{-4} \pm 5 \times 10^{-5}$.

The dynamic flow birefringence (dynamo-optical Maxwell effect) was studied in a dynamo-optimeter with an inner rotor 3 cm in diameter and 3.21 cm in height. The gap between the stator and the rotor was 0.022 cm. To enhance the sensitivity, we used a photoelectric detection circuit with modulation of the light polarization ellipticity [27,32] and a semiconductor laser (HLDPM 12.655.5, wavelength $\lambda \approx 655$ nm) as a light source. The elliptical rotary compensator provided the relative path difference $\Delta\lambda/\lambda = 0.04$. The flow birefringence was studied at a temperature of 24 °C maintained by forced water thermostating of the device. The error of the determination of the optical shear coefficient when using the above technique did not exceed 10% and was caused mainly by possible uncertainties in determination of the flow velocity gradient and in measurements of the dynamo-optimeter geometry, as well as by variations in the temperature at which the experiments were carried out.

3. Results and discussion

Viscometry was used to obtain concentration dependences of reduced viscosity η_r of the synthesized samples; some of them are presented in Fig. 4. Extrapolation of dependences to infinite dilution allowed us to determine values of intrinsic viscosity of macromolecules $[\eta]$; using slope of lines, it is possible to calculate the Huggins constants K' according to the relationship

$$\eta_r = [\eta] + K'[\eta]^2 c \quad (3)$$

The obtained data are presented in Table 1. The intrinsic viscosity values lie in the range from 20 to 140 cm^3/g. The average K' value is close to 0.4, which indicates that the two-component solvent $D + C$ is thermodynamically close to ideal (θ-conditions).

The relaxation time distributions obtained from autocorrelation function of scattered light intensity for all the studied samples (except Sample 4) demonstrate two peaks (Fig. 5). The main peak corresponds to the translational diffusion of individual PAADA molecules, and the second one can be apparently attributed to the diffusion of macromolecular aggregates. Estimation of contributions made by second components for a number of samples showed that 3–5% of this second component is present in samples.

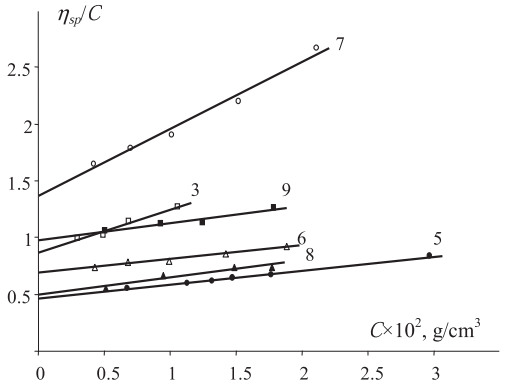

Fig. 4. Concentration dependences of reduced viscosity η_{sp}/C for different PAADA samples in the mixed solvent ($D + C$): 3, 5, 6, 7, 8, 9 numbers.

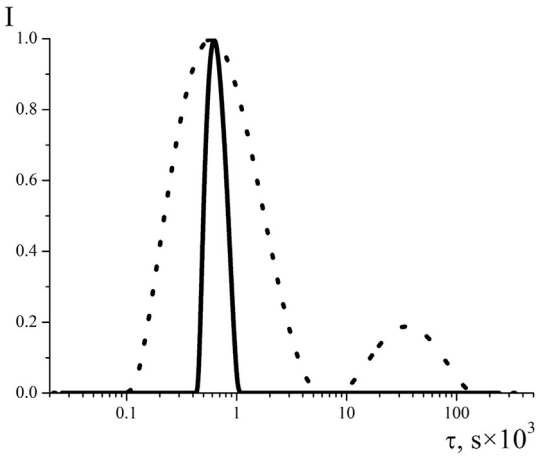

Fig. 5. Normalized scattered light intensity distribution: solid line – PAADA-4; dashed line – PAADA-3.

However, even this low concentration of the second component led to considerable distortion in the data obtained by static light scattering. The deviations of the measured light scattering intensity at identical q were about 70% of the average value. The determined molecular masses values were significantly overstated [31]. The angular dependence of R_θ was practically absence. The radius of gyration value R_g could not be determined with sufficient precision under the conditions of this experiment.

The dependences of inverse relaxation time $1/\tau$ on square of wave vector (q^2) are linear and pass through the origin of coordinates (Fig. 6a). Translational diffusion coefficients D_c were calculated from slopes of these lines. Extrapolation of concentration dependences of D_c to infinite dilution (Fig. 6b) allowed us to determine diffusion coefficients D of PAADA macromolecules (Table 1).

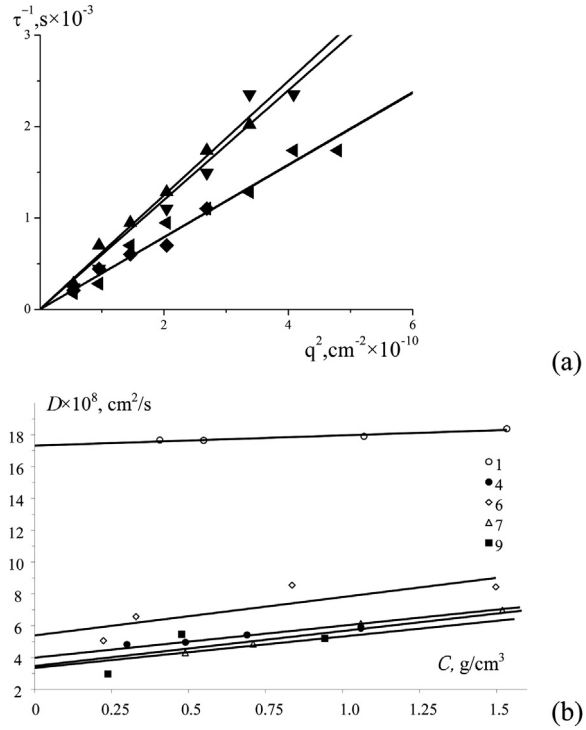

Fig. 6. (a) The dependence of inverse relaxation time $1/\tau$ on the square of wave vector q^2 for PAADA sample 4 in the mixed solvent ($D + C$); and (b) concentration dependence of diffusion coefficient D_c of different PAADA samples.

It should be emphasize that only for one sample of the polymer under investigation (the PAADA-4) the relaxation time distributions function, obtained from dynamic light scattering measurements, revealed a complete absence of the second peak associated with macromolecular aggregates diffusion. For PAADA-4 sample, using the static light scattering data, molecular mass M_w was found to be 65×10^4, and the second virial coefficient A_2 was equal to 3.7×10^{-4} ml $\times$ mol/g^2.

To refine molecular mass of the PAADA-4 sample, sedimentation velocity method was used. Sedimentation coefficients (s) in the mixed solvent D + C (25 °C) were measured using an analytical ultracentrifuge ProteomeLab XL-I (Beckman Coulter, USA). In the experiments, four-hole titanium rotor and cells with two-sector aluminum centerpieces were used. Sedimentation was observed at a rotation speed of 40×10^3 rpm. The obtained data (concentration distribution in cells depending on sedimentation time) were processed by SedFit software using the continuous $C(s)$ distribution model [33,34].

The extrapolation of sedimentation coefficients s to infinite dilution was made (Fig. 7); the concentration varied in the range from 0.15 to 0.5×10^{-2} g/cm^3. The obtained values of diffusion coefficients D and sedimentation coefficients s_0 were used to calculate molecular mass of the sample 57×10^4 by means of the Svedberg equation $M_{SD} = RT(s_0 \cdot D^{-1})(1 - \overline{V}\rho_0)^{-1}$. The partial specific volume of the polymer $\overline{V} = 0.9334$ cm^3/g was determined from the concentration dependence of density measured with the aid of a DMA 5000 M density meter (Anton Paar).

It can be seen that the values of M_w and M_{SD} for the PAADA-4 sample calculated from static light scattering and sedimentation velocity data are comparable. The average value of M for sample 4 (Table 1) was used to calculate hydrodynamic invariant A_0 by the formula

$$A_0 = \frac{\eta_0 D (M[\eta])^{1/3}}{T}. \quad (4)$$

The calculated value $A_0 = 3.22 \times 10^{-10}$ erg/K is close to the average value of hydrodynamic invariant $A_0 = 3.26 \times 10^{-10}$ erg/K calculated in Ref. [28] for PAAUA samples. For further calculations of molecular masses, we used the first value ($A_0 = 3.22 \times 10^{-10}$ erg/K). Table 1 gives molecular masses of polymers calculated by means of Eq. (4) using $[\eta]$ and D values. The M values of the studied polymers range from 0.8×10^5 to 12.6×10^5.

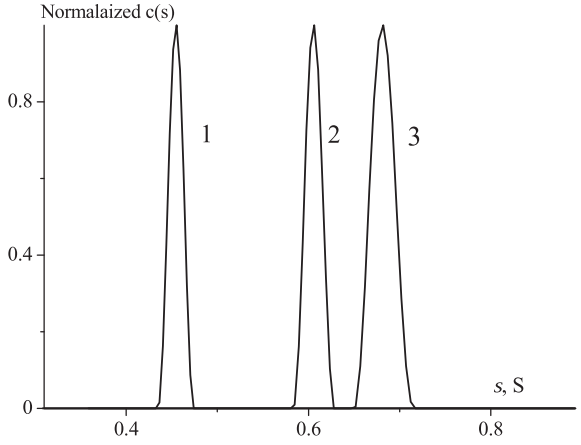

Fig. 7. Differential distribution of the sedimentation coefficients for the PAADA sample 4 in the mixed solvent ($D + C$) at different concentrations $c \times 10^3$ g/cm^3: 5.14 (1), 2.69 (2), 1.45 (3). The acquired sedimentation data were used for evaluation of sedimentation coefficient s_0 at infinite dilution.

Fig. 8 shows the dependences of lg[η] and (lg($\eta_0 D$) + 11) on lg M for PAADA samples. The Mark–Kuhn–Houwink equations for the D + C mixture (1:1) within the molecular mass range of (0.8–12.6) $\times 10^5$ take the form:

$$[\eta] = 0.083 \times M^{0.5}$$
$$\eta_0 D = 1.05 \times 10^{-6} M^{-0.5} \quad (5)$$

The exponent values in these equations are typical of polymers with rather low equilibrium rigidity and high molecular mass in the absence of volume effects (i.e. in θ-conditions).

Fig. 9 demonstrates the dependences of η_0DM/RT on $M^{1/2}$ which can be plotted as straight lines according to the following equation [35]:

$$\eta_0 DM/RT = (PN_A)^{-1}(M_0/\lambda A)^{1/2} M^{1/2} + (M_0/3\pi N_A \lambda) \times [\ln(A/d) - 1.0561], \quad (6)$$

where M_0 is the molecular mass of a repeating unit; $\lambda = 2.5 \times 10^{-8}$ cm is the length of a repeating unit; A is the Kuhn segment length; d is the chain diameter; η_0 is the solvent viscosity; $P = 5.11$ is the theoretical constant; the rest of designations are universally accepted. Fig. 9 also shows data for PAAUA samples (dashed line). The slope of linear dependence allows to obtain the Kuhn segment length $A = 62 \times 10^{-8}$ cm, and hydrodynamic diameter $d = 34 \times 10^{-8}$ cm was determined from the Y-axis intercept. The hydrodynamic diameter value for PAADA correlates with the structure of macromolecules far better than the value obtained earlier for PAAUA ($d = 45 \times 10^{-8}$ cm) [29].

The density of polymer sample PAADA-1 was measured ($\rho = 1.0058$ g/cm^3), the partial specific volume of the polymer was calculated using the relationship $\overline{V} = 1/\rho$ and found to be 0.9942 cm^3/g. The obtained data have also allowed us to calculate hydrodynamic diameter by the formula $d = \sqrt{4M_0\overline{V}/\pi\lambda N_A} = 15 \times 10^{-8}$ cm. The calculated hydrodynamic diameter of polymer chain is two times less than the diameter calculated from the relationship (6), this indicating possible overstating the percolation effect when using the traditional wormlike spherocylinder model [35]. The presence of a considerable amount of long side groups in macromolecules leads to increase in translational friction of polymer chains and, as a result, to increase in their hydrodynamic diameter d.

The value of equilibrium rigidity of PAADA macromolecules is higher than that of the majority of comb-shaped polymers [22]. Apparently, increased equilibrium rigidity of PAAUA and PAADA macromolecules is caused not only by steric interactions (repulsion) between side groups, but also by interactions between amide fragments in these groups (hydrogen bond formation, in the first place). These interactions lead to the formation of “quasi-ladder”

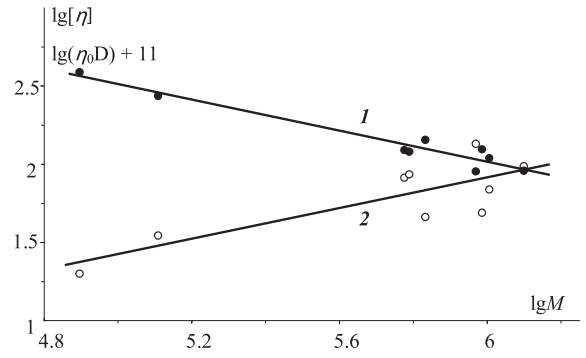

Fig. 8. The dependences of lg ($\eta_0 D$) (1) and lg[η] (2) on lg$M$ for PAADA samples in the mixed solvent ($D + C$).

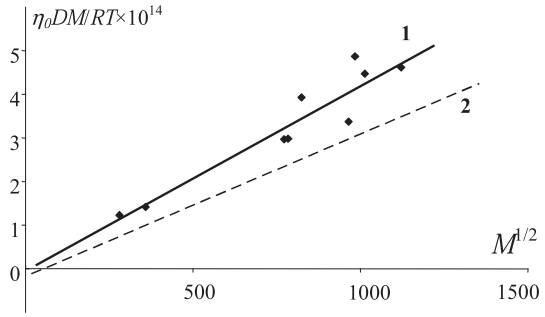

Fig. 9. The dependences of $\eta_0 DM/RT$ on $M^{1/2}$ for PAADA (1) and PAAUA (2) samples in the mixed solvent ($D + C$).

structure in macromolecules and, therefore, to increased equilibrium rigidity as compared with that of aliphatic comb-shaped polyacrylates and polymethacrylates [22].

Optical properties of PAADA molecules were studied using flow birefringence in mixed solvent. Fig. 10 presents the dependence of flow birefringence Δn on flow rate gradient g for PAADA-4 sample in the mixed solvent at various polymer concentrations. It can be seen that all experimental data can be well extrapolated by straight lines. Similar results were observed for other polymer studied. Fig. 11 shows dependences of flow birefringence Δn on shear stress $\Delta\tau$ for PAADA samples 3, 4, 6 and 7. It is apparent that all experimental data are well extrapolated by straight lines passing through the origin of coordinates, this picture being characteristic of true solutions. From the slope of the line, it is possible to determine optical shear coefficient $\Delta n/\Delta\tau$. The average value of optical shear coefficient for PAADA is $\Delta n/\Delta\tau_{av} = -4.5 \times 10^{-10}$ cm $\times$ s^2/g.

This value is close to the one obtained after measurements in the same solvent for PAAUA ($\Delta n/\Delta\tau_{av} = -4.7 \times 10^{-10}$ cm $\times$ s^2/g). This coincidence is regular and results from closeness between optical (optical anisotropy of monomer unit) and conformational (equilibrium rigidity of macromolecules) characteristics of PAAUA and PAADA.

Let us consider in more detail the results of dynamo-optical measurements obtained in the mixed solvent. Optical shear coefficient $\Delta n/\Delta\tau$ for the systems with differing refractive indices of polymer and solvent can be presented as a sum of three terms [22]:

$$\Delta n/\Delta\tau = (\Delta n/\Delta\tau)_i + (\Delta n/\Delta\tau)_{fs} + (\Delta n/\Delta\tau)_f \quad (7)$$

The first term represents the contribution made by the intrinsic optical anisotropy of molecules, the second and third terms characterize contributions made by anisotropies of micro- and macroform, respectively.

The terms in the Eq. (7) can be presented as [22]:

$$\left(\frac{\Delta n}{\Delta\tau}\right)_i = \frac{4\pi(n_s^2+2)^2}{45kTn_s} \times (\alpha_1 - \alpha_2)_i, \quad (8)$$

$$\left(\frac{\Delta n}{\Delta\tau}\right)_{fs} = \frac{(n_s^2+2)^2\left(2n_s\rho\frac{dn}{dc}\right)^2}{180\pi RTn_s^3\rho} \times M_A(L_2 - L_1)_s, \quad (9)$$

$$\left(\frac{\Delta n}{\Delta\tau}\right)_f = \frac{0.058\Phi(n_s^2+2)^2\left(2n_s\rho\frac{dn}{dc}\right)^2}{\pi\rho^2 N_A RTn_s^3} \times \frac{M}{[\eta]}, \quad (10)$$

where M_A is the molecular mass of the Kuhn segment; $(L_2 - L_1)$ is the asymmetry parameter of the segment; Φ is the Flory constant; N_A is the Avogadro number.

The relationships (8)–(10) are applicable only for chains which are coiled to a certain degree. In our studies, all samples (1)–(9) satisfied this condition. In calculating the contribution of microform effect $(\Delta n/\Delta\tau)_{fs}$, the value $M_A = 6650$ was used. As evidenced by the data of hydrodynamic studies in the mixed solvent, segment axes ratio for PAADA (A/d) is close to 2. This value of the A/d parameter corresponds to the segment asymmetry parameter $(L_2 - L_1)_s = 3$ [Formula (5.24) [22]]. The $(\Delta n/\Delta\tau)_{fs}$ value was calculated (4.9×10^{-10} cm $\times$ s^2/g). In calculating the contribution of macroform effect, the value of the Flory coefficient was accepted to be 2.1×10^{23}. During calculating both effects, we used the average value of refractive index increment $dn/dc = (0.085 \pm 0.015)$ cm^3/g. The obtained values of macroform effect are presented in Table 2.

In the last column of Table 2, the values of optical shear coefficient $(\Delta n/\Delta\tau)_i$ are given calculated with consideration for macro- and microform effects. We have estimated intrinsic optical anisotropy of the molecular segment $(\alpha_1 - \alpha_2)_i = -202 \times 10^{-25}$ cm^3 for samples with the highest molecular masses by means of the Kuhn relationship (8). Using the value of equilibrium rigidity obtained from hydrodynamic data ($A = 62 \times 10^{-8}$ cm), we have found the value of intrinsic anisotropy of polarizability for the monomer unit $(a_{||} - a_{\perp}) = \Delta a_i$; it is equal to -8.15×10^{-25} cm^3.

The obtained optical characteristics of PAADA in the mixed solvent can be compared with those for comb-shaped polyalkylacrylates with side chains of similar length. Thus, for poly(-decylacrylate) with 12 bonds in side chain, in the solvent with zero refractive index increment, where contributions of macro- and microform effects to the measured birefringence are absent, $\Delta n/$

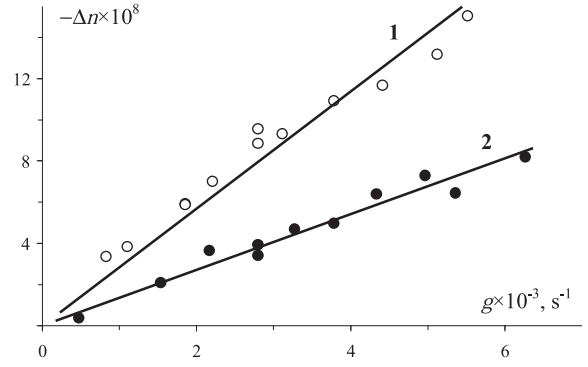

Fig. 10. The dependence of flow birefringence Δn on flow rate gradient g for PAADA-4 sample in the mixed solvent ($D + C$); concentration $c \times 10^2$ (g/cm^3) is 1.41 (1) and 0.78 (2).

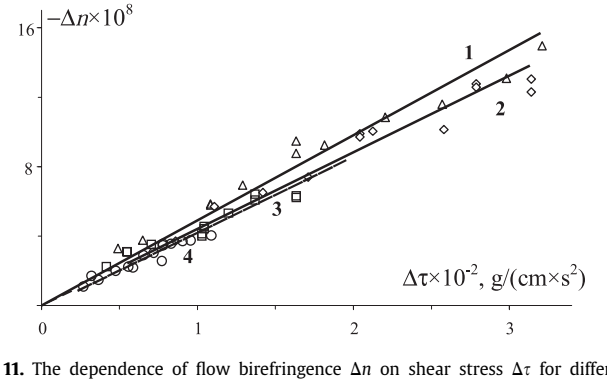

Fig. 11. The dependence of flow birefringence Δn on shear stress $\Delta\tau$ for different PAADA samples in the mixed solvent ($D + C$); 1 – sample 4; 2 – sample 7; 3 – sample 3; and 4 – sample 6. Concentration $c \times 10^2$ (g/cm^3): 1 – 1.4, 2 – 1.1, 3 – 0.75, and 4 – 0.95.

Table 2
Optical characteristics of PAADA in the mixed solvent ($D + C$) at 24 °C.

Ser. No.	$M \times 10^{-4}$	$[\eta]$, cm^3/g	dn/dc	$\Delta n/\Delta\tau \times 10^{10}$, $cm \times s^2/g$	$(\Delta n/\Delta\tau)_f \times 10^{10}$, $cm \times s^2/g$	$(\Delta n/\Delta\tau)_i \times 10^{10}$, $cm \times s^2/g$
2	13	35	0.10	−8.1	3.2	−16.0
3	60	82	0.07	−4.4	6.3	−15.5
4	61	86	0.07	−4.9	6.2	−16.0
6	90	69	0.10	−4.2	11.2	−20.2
7	93	135	–	−4.4	5.9	−15.2

$\Delta\tau = -7.7 \times 10^{-10}$ cm × s^2/g, $(\alpha_1 - \alpha_2) = -95 \times 10^{-25}$ cm^3 and $(a_{||} - a_{\perp}) = \Delta a_i = -4.7 \times 10^{-25}$ cm^3 [22]. Therefore, absolute value of anisotropy of optical polarizability for the PAADA monomer unit is somewhat higher than that for poly(decylacrylate). The rigidity of the PAADA main chain is also considerably higher than that of polyethylene chain; this effect may be caused by interactions between side moieties as well as the formation of hydrogen bond in the side group. It is interesting to estimate rigidity of side chains in PAADA macromolecules.

The side radical of a comb-shaped molecule can be considered as a wormlike chain with the first unit being rigidly bound to the backbone and square with it. The monomer unit anisotropy of comb-shaped PAADA molecule can be calculated as

$$\Delta a_i = 2\Delta b - \left[\Delta b \cdot \nu\left(1 - e^{-6n/\nu}\right)/12\right] - \Delta\gamma_{CONH}, \qquad (11)$$

where $\Delta\gamma_{CONH} = -4.1 \times 10^{-25}$ cm^3 is the estimating value of amide group contribution obtained using HyperChem software; Δb is the anisotropy of C–C bond polarizability; ν is the number of valence bonds in the Kuhn segment of the side chain; $n = 12$ is the number of valence bonds in the side chain. In estimating the ν value for PAADA, we use the experimental value of optical anisotropy for one valence C–C bond in polyethylene chain as Δb.

Using the experimental values of Δb $(3.0–3.3) \times 10^{-25}$ cm^3 [22,28] results in $\nu \approx 55–60$. For alkyl esters of polymethacrylic acid in benzene and for polyalkylacrylates in toluene and decalin solutions, $\Delta b = (2.6–3.3) \times 10^{-25}$ cm^3 and ν is about 60–80 ([22] pp. 292–293). It is apparent that the results obtained for PAADA are in good agreement with polyalkylacrylates and polyalkylmethacrylates data, with the calculated ν values being 4–5 times higher than the polyethylene rigidity parameter ($\nu = 16$). To summarize, the enhanced rigidity of PAADA side chains indicates the presence of orientational order which far exceeds conformational order of flexible polymer chains. This phenomenon may be caused by interactions between side chains which are located rather closely in comb-shaped macromolecules and is in agreement with theoretical predictions and results of computer simulations for comb-like polymers [36–39]. Besides, this interaction manifests itself stronger in the case of long side alkyl groups and results in both some decrease in the flexibility of the main chain and considerable increase in rigidity and optical anisotropy of side chains.

4. Conclusions

In the present work, comprehensive studies of comb-shaped poly(12-acryloylaminododecanoic acid) samples with molecular masses ranging from 0.8×10^5 to 12.6×10^5 were performed using molecular hydrodynamics and optical methods. The main conformational characteristics of macromolecules were determined: equilibrium rigidity $A = 62 \times 10^{-8}$ cm and effective hydrodynamic diameter $d = 34 \times 10^{-8}$ cm. The obtained values of exponents in the Mark–Kuhn–Houwink equations for translational friction coefficient and intrinsic viscosity are close to 0.5. These values are typical of polymers with moderate equilibrium rigidity and rather high molecular mass in the absence of noticeable volume effects (the last fact agrees with the obtained values of the Huggins constants K').

The average experimental value of optical shear stress coefficient for PAADA is $\Delta n/\Delta\tau_{av} = -4.5 \times 10^{-10}$ cm × s^2/g. This is close to the result obtained earlier for PAAUA in the same solvent ($\Delta n/\Delta\tau_{av} = -4.7 \times 10^{-10}$ cm × s^2/g). The coincidence is regular and results from closeness between optical (optical anisotropy of monomer unit) and conformational (equilibrium rigidity of macromolecules) characteristics of PAAUA and PAADA.

The detailed analysis of contributions of optical microform and macroform effects to the observed flow birefringence was performed; the value of intrinsic optical anisotropy of monomer unit was determined ($\Delta a_i = -8.15 \times 10^{-25}$ cm^3). It was concluded that interactions between side chains lead not only to increasing equilibrium rigidity of PAADA backbone, but also to increase in rigidity and optical anisotropy of side chains in macromolecules.

Acknowledgments

This work was supported by the Russian Foundation for Basic Research (projects number 12-03-00687 and 13-03-00474). The studies were carried out using the instruments of the Analytical Resource Center of Saint-Petersburg State University “Centre for diagnosis of functional materials in medicine, pharmacology and nanoelectronics”.

References

[1] Rodrıguez JL, Schulz PC, Pieroni O, Vuano B. Colloid Polym Sci 2004;282(7):734–9. http://dx.doi.org/10.1007/s00396-003-1005-z.
[2] Larrabee CE, Spargue ED. J Polym Sci C Polym Lett 1979;17(12):749–51. http://dx.doi.org/10.1002/pol.1979.130171201.
[3] Hartmann PC, Lupo M, Weber W, Sanderson RD. Macromol Symp 2006;231(1):94–102. http://dx.doi.org/10.1002/masy.200590029.
[4] Yeoh KW, Chew CH, Gan LM, Koh LL. Polym Bull 1989;22(2):123–9. http://dx.doi.org/10.1007/BF00255201.
[5] Roy S, Dey J. Langmuir 2003;19(23):9625–9. http://dx.doi.org/10.1021/la0348113.
[6] Yeoh KW, Chew CH, Can LM, Koh LL, Teo HH. J Macromol Sci – Pure Appl Chem A 1989;26(4):663–80. http://dx.doi.org/10.1080/00222338908052001.
[7] Fujimoto C, Fujise Y, Kawaguchi S. J Chromatogr A 2000;871(1–2):415–25. http://dx.doi.org/10.1016/S0021-9673(99)00848-1.
[8] Samakande A, Hartmann PC, Sanderson RD. J Colloid Interface Sci 2006;296(1):316–23. http://dx.doi.org/10.1016/j.jcis.2005.09.005.
[9] Hamid SM, Sherrington DC. Polymer 1987;28(2):325–31. http://dx.doi.org/10.1016/0032-3861(87)90426-5.
[10] Egorov VV. J Polym Sci A 1995;33(10):1727–33. http://dx.doi.org/10.1002/pola.1995.080331020.
[11] del J Gutiérrez-Hijar DP, Becerra F, Puig JE, Soltero-Martínez JFA, Sierra MB, Schulz PC. Colloid Polym Sci 2004;283(1):74–83. http://dx.doi.org/10.1007/s00396-004-1094-3.
[12] Cochin D, Zana R, Candau F. Polym Int 1993;30(4):491–8. http://dx.doi.org/10.1002/pi.4990300412.
[13] Summers M, Eastoe J, Davis S, Du Z, Richardson RM, Heenan RK, et al. Langmuir 2001;17(17):5388–97. http://dx.doi.org/10.1021/la010541h.
[14] Hartmann PC, Sanderson RD. Macromol Symp 2005;225(1):229–37. http://dx.doi.org/10.1002/masy.200550718.
[15] Paleos CM, Stassinopoulou CI, Malllaris A. J Phys Chem 1983;87(2):251–4. http://dx.doi.org/10.1021/j100225a016.
[16] Arai K, Maseki Y, Ogiwara Y. Macromol Chem Rapid Commun 1987;8(11):563–7. http://dx.doi.org/10.1002/marc.1987.030081109.
[17] Cochin D, Candau F, Zana R. Macromolecules 1993;26(21):5755–64. http://dx.doi.org/10.1021/ma00073a033.

[18] Nayak RR, Roy S, Dey J. Colloid Polym Sci 2006;285(2):219–24. http://dx.doi.org/10.1007/s00396-006-1554-z.
[19] Kline SR. J Appl Cryst 2000;33(3):618–22. http://dx.doi.org/10.1107/S0021889899012753.
[20] Gerber MJ, Kline SR, Walker LM. Langmuir 2004;20(20):8510–6. http://dx.doi.org/10.1021/la048929a.
[21] Kuntz DM, Walker LM. J Phys Chem B 2007;111(23):6417–24. http://dx.doi.org/10.1021/jp0688308.
[22] Tsvetkov VN. Rigid-chain polymers. London: Consult Bur Plenum NY; 1989.
[23] Szczubiałka K, Nowakowska M. Polymer 2003;44(18):5269–74. http://dx.doi.org/10.1016/S0032-3861(03)00479-8.
[24] Nayak RR, Roy S, Dey J. Polymer 2005;46:12401–9. http://dx.doi.org/10.1016/j.polymer.2005.10.127.
[25] Dutta P, Dey J, Ghosh G, Nayak RR. Polymer 2009;50:1516–25. http://dx.doi.org/10.1016/j.polymer.2008.12.049.
[26] Koňák Č, Ganchev B, Teodorescu M, Matyjaszewski K, Kopečková P, Kopeček J. Polymer 2002;43(13):3735–41. http://dx.doi.org/10.1016/S0032-3861(02)00182-9.
[27] Tsvetkov VN [chapter 14]. In: Ke B, editor. Newer methods of polymer characterization. New York: Interscience; 1964. pp. 563–665.
[28] Tsvetkov VN, Andreeva LN [chapter 4]. In: Brandrup J, Immergut EH, editors. Polymer handbook. New Lork: Wiley Interscience; 1975. pp. 377–85.
[29] Tsvetkov NV, Andreeva LN, Lebedeva EV, Strelina IA, Lezov AA, Podseval'nikova AN, et al. Polym Sci A 2011;53(8):666–77. http://dx.doi.org/10.1134/S0965545X11080104.
[30] Roy S, Dey J. Langmuir 2003;19(23):9625–9. http://dx.doi.org/10.1021/la0348113.
[31] Wu C, Siddiq M, Woo KF. Macromolecules 1995;28(14):4914–9. http://dx.doi.org/10.1021/ma00118a019.
[32] Tsvetkov VN, Andreeva LN. Adv Polym Sci 1981;39:95–207. http://dx.doi.org/10.1007/3-540-10218-3_3.
[33] Schuck P. Biophys J 2008;78(3):1606–19. http://dx.doi.org/10.1016/S0006-3495(00)76713-0.
[34] www.analyticalultracentrifugation.com.
[35] Yamakawa H. Macromolecules 1977;10(3):692–6. http://dx.doi.org/10.1021/ma60057a039.
[36] Feuz L, Leermakers FAM, Textor M, Borisov O. Macromolecules 2005;38(21):8891–901. http://dx.doi.org/10.1021/ma050871z.
[37] Saariaho M, Ikkala O, Szleifer I, Erukhimovich I, ten Brinke G. J Chem Phys 1997;107(8):3267–76. http://dx.doi.org/10.1063/1.474677.
[38] Saariaho M, Szleifer I, Ikkala O, ten Brinke G. Macromol Theory Simul 1998;7(2):211–6. http://dx.doi.org/10.1002/(SICI)1521-3919(19980301)7:2<211::AID-MATS211>3.0.CO;2-A.
[39] Subbotin A, Saariaho M, Ikkala O, ten Brinke G. Macromolecules 2000;33(9):3447–52. http://dx.doi.org/10.1021/ma991031l.